Since January 2020 Elsevier has created a COVID-19 resource centre with free information in English and Mandarin on the novel coronavirus COVID-19. The COVID-19 resource centre is hosted on Elsevier Connect, the company's public news and information website.

Talanta 248 (2022) 123594

Contents lists available at ScienceDirect

Talanta

journal homepage: www.elsevier.com/locate/talanta

Automated, portable, and high-throughput fluorescence analyzer (APHF-analyzer) and lateral flow strip based on CRISPR/Cas13a for sensitive and visual detection of SARS-CoV-2

Gaihua Cao [a], Danqun Huo [a,b], Xiaolong Chen [a], Xianfeng Wang [a], Shiying Zhou [a], Shixian Zhao [b,c,**], Xiaogang Luo [a,***], Changjun Hou [a,*]

[a] Key Laboratory of Biorheological Science and Technology of Ministry of Education, State and Local Joint Engineering Laboratory for Vascular Implants, Bioengineering College of Chongqing University, Chongqing, 400044, PR China
[b] Chongqing Key Laboratory of Bio-perception & Intelligent Information Processing, School of Microelectronics and Communication Engineering, Chongqing University, Chongqing, 400044, PR China
[c] Chongqing Engineering and Technology Research Center of Intelligent Rehabilitation and Eldercare, Chongqing City Management College, Chongqing, 401331, China

ARTICLE INFO

Keywords:
SARS-CoV-2
CRISPR/Cas13a
Recombinase polymerase amplification (RPA)
Lateral flow strip
Point of care testing (POCT)
On-site detection

ABSTRACT

COVID-19 has erupted and quickly swept across the globe, causing huge losses to human health and wealth. It is of great value to develop a quick, accurate, visual, and high-throughput detection of severe acute respiratory syndrome coronavirus 2 (SARS-CoV-2). Here, we developed a biosensor based on CRISPR/Cas13a combined with recombinase polymerase amplification (RPA) to detect S and Orf1ab genes of SARS-CoV-2 within 30 min. Most important of all, we developed an automated, portable, and high-throughput fluorescence analyzer (APHF-analyzer) with a 3D-printed microfluidic chip for sensitively detecting SARS-CoV-2, which addressed aerosol contamination issue and provided a more accurate and high-throughput detection during the on-site detection process. The detection limits of S gene and Orf1ab gene were as low as 0.68 fM and 4.16 fM. Furthermore, we used the lateral flow strip to realize visualization and point of care testing (POCT) of SARS-CoV-2. Therefore, profit from the efficient amplification of RPA and the high specificity of CRISPR/Cas13a, APHF-analyzer and the lateral flow strip to simultaneous detection of S gene and Orf1ab gene would be applied as a promising tool in the field of SARS-CoV-2 detection.

Author statement outlining

Gaihua Cao: Conceptualization, Methodology, Writing - Original Draft, Writing - Review & Editing. Danqun Huo: Methodology and Formal analysis. Xiaolong Chen: Methodology and Formal analysis. Xianfeng Wang: Formal analysis. Shiying Zhou: Methodology and Formal analysis. Shixian Zhao: Formal analysis. Xiaogang Luo: Formal analysis. Changjun Hou: Writing - Review & Editing, Project administration, Funding acquisition.

1. Introduction

COVID-19 caused by severe acute respiratory syndrome-coronavirus 2 (SARS-CoV-2) has brought great disaster to the whole world. SARS-CoV-2 spreads quickly [1,2], even it has been found in wastewater [3,4]. And the symptoms caused by SARS-CoV-2 are so similar to other pneumonia that it is hard to tell apart [5]. Therefore, a specific SARS-CoV-2 detection method with simple operation, high throughput, sensitivity, and accuracy is urgently needed to effectively cope with the crisis. Common SARS-CoV-2 detection methods include immunoassay [6] and nucleic acid assay [7]. Immunoassay is accurate, but it suffers from some disadvantages in low sensitivity and certain hysteresis [8,9],

* Corresponding author.
** Corresponding author. Chongqing Engineering and Technology Research Center of Intelligent Rehabilitation and Eldercare, Chongqing City Management College, Chongqing, 401331, China.
*** Corresponding author.
E-mail addresses: 20161901031@cqu.edu.cn (S. Zhao), 13400818@qq.com (X. Luo), houcj@cqu.edu.cn (C. Hou).

https://doi.org/10.1016/j.talanta.2022.123594
Received 14 August 2021; Received in revised form 13 March 2022; Accepted 25 May 2022
Available online 27 May 2022

which limit its wide application. On the contrary, nucleic acid detection is more sensitive and timely. The gold standard of nucleic acid testing is real-time quantitative PCR [10,11]. But it requires trained operators, expensive equipment, and certified laboratories, which still has great difficulties in remote areas where lack of resources and medical facilities. Hence, it is of great value to invent a portable and high-throughput method to suit to point of care test (POCT).

SARS-CoV-2 gene is a positive single-stranded RNA [12,13]. Though the virus escapes from the immune system with a high mutation in the process of human-to-human transmission [14], SARS-CoV-2 has some highly conserved domains, such as S gene, Orf1ab gene. To avoid false-positive or false-negative for only testing one gene, we decided to test the S gene and Orf1ab gene at the same time to increase specificity and accuracy. Amplified areas and sequences were shown in Fig. S5 (Supporting information). Because the content of the SARS-CoV-2 gene is very few after gene extraction from the samples collected, some amplification methods are needed to augment the concentration to adjust to existing detection methods. For example, rolling circle amplification (RCA) [15], loop-mediated isothermal amplification (LAMP) [16,17], strand displacement amplification (SDA) [18], polymerase chain reaction (PCR) [7,19], Nucleic acid sequence-based amplification (NASBA) [20], recombinase polymerase amplification (RPA) [21,22]. Among them, RPA is a relatively mature isothermal amplification technology with high amplification efficiency and high specificity. It can be amplified a million times in 5–20 min.

With the advent of the clustered regularly interspaced short palindromic repeats (CRISPR)/associated protein (Cas) system, the detection industry ushered in new development due to its rapid and precise cutting capability. So far, CRISPR/Cas9 [23], CRISPR/Cas12 [24,25], CRISPR/Cas13 [26,27], and CRISPR/Cas14 [28] system have been discovered. For instance, James P developed a strategy based on RT-LAMP and CRISPR/Cas12a to detect the E and N gene of SARS-CoV-2 in 40 min, with a limit of detection (LOD) of 1 copy per sample [29]. Lu exploited the CASdetec (CRISPRassisted detection) platform combining recombinase-assisted amplification (RAA) with Cas12 b to detect the RdRp gene of SARS-CoV-2, with the LOD as low as 1×10^4 copies·mL^{-1} [30]. Yong invented a cascade CRISPR/Cas (casCRISPR) system by the *trans*-cleavage activity of Cas13a and Cas14a to detect miRNA with a LOD of 1.33 fM [31]. Among them, CRISPR/Cas13a system has attracted extensive attention in biochemical sensing, especially RNA detection, owing to its high specificity and *trans*-cleavage activity to RNA. To be specific, it specifically identifies and combines the RNA target by hybridization with the crRNA. After that, the *trans*-cleavage activity of Cas13a is activated by RNA to discretionarily cut nonspecific RNA [32]. Huang made full use of the high efficiency of hyper-branching rolling circle amplification as well as robust collateral cleavage activity of Cas13a to build a HyperCas platform for microRNA-17. It achieved a LOD of 200 aM [33]. Parinaz designed multiple crRNA to bind to RNA of SARS-CoV-2 to rapidly activate the *trans*-cleavage activity of Cas13a for generating fluorescent signals. This method did not require nucleic acid amplification and had a LOD of 100 copies·mL^{-1} by mobile phone microscopy [34]. In conclusion, the CRISPR/Cas13a system is suitable for specific and sensitive detection.

Currently, many portable instruments have been developed to achieve POCT. For example, portable devices used a simple fluorescent lamp in conjunction with a smartphone based on isothermal amplification to test DNA or RNA [35,36], but they still required additional heating devices. In addition, judging negative or positive by simple fluorescence brightness will lead to false negative phenomenon due to environmental factors. They can be for preliminary screening because they are not accurate enough. Other precision devices include temperature control systems and signal detection systems, but they were cumbersome and high-cost [37].

In this paper, we developed an automatic, portable, and high-throughput fluorescence analyzer (APHF-analyzer) with a microfluidic chip and lateral flow strip based on CRISPR/Cas13a technology with RPA strategy for sensitively and specifically detecting S gene and Orf1ab gene of SARS-CoV-2. Through taking full advantage of two technologies by APHF-analyzer, it was satisfactory that LOD of the S gene was 0.68 fM and Orf1ab gene as 4.16 fM in 30 min. In comparison, by LS-55 spectrophoto fluorometer (commercially available fluorescence meter), the LOD of the S gene and Orf1ab gene were 9.2 fM and 17.2 fM, illustrating that APHF-analyzer has greater potential to be applied in the actual detection of SARS-CoV-2. And the APHF-analyzer with a microfluidic chip was designed to realize high-throughput detection of SARS-CoV-2 for POCT. In addition, in order to achieve visual detection, we used lateral flow strips to detect the S gene and Orf1ab gene. And the LOD reached 2 fM and 20 fM, respectively. In conclusion, it is no exaggeration to say that the biosensor based on CRISPR/Cas13a technology and RPA strategy, detected by lateral flow strip and the APHF-analyzer, will have great potential in coping with COVID-19.

2. Materials and methods

2.1. Reagents and instrumentations

All oligonucleotides sequences were shown in Table S1 (Supporting information). Template oligonucleotide sequences and the plasmid of SARS-CoV, human RPP30 (Hs-RPP30), and Middle East respiratory syndrome coronavirus (MERS-CoV) were purchased from Sangon Biotech (Shanghai, China), and other oligonucleotide sequences were synthesized by ourselves. MiRcute miRNA Isolation Kit (DP501) and DNase/RNase-free water were purchased from TIANGEN Biotechnology Co. The T7 Mix (MAXI 100), Taq DNA polymerase (5000 U·mL^{-1}), DNase I (2000 U·mL^{-1}), 10 × DNase I buffer, 10 × NEB buffer 2.1, ProtoScript® II Reverse Transcriptase (10 000 U·mL^{-1}), T7 RNA polymerase (50 000 U·mL^{-1}), and RNA inhibitor (40 000 U·mL^{-1}) were ordered from New England Biotechnology Co., Ltd (Beijing, China). The RPA kit was supplied by TwistDx (Cambridge, UK). LwCas13a (100 μM) protein was ordered from Beijing Kesin Biotechnology Co., LTD. Universal lateral flow dipstick for detection of biotin- and FITC-labeled analytes was bought from Milenia Biotec (Germany).

2.2. Synthesis RNA targets of S gene and Orf1ab gene

Because long RNA was difficult to synthesize, we used PCR combined with in vitro transcription method to synthesize RNA of the S gene and Orf1ab gene. The principle of synthesis could be seen in Fig. S1 (Supporting information). The 20 μL reaction solution containing 10 μM forward primer T7-S gene-F or T7-Orf1ab gene-F, 10 μM reverse primer S gene-R or Orf1ab gene-R, 25 mM dNTP and 5000 U Taq DNA polymerase was conducted 30 thermal cycles, 95 °C for 20 s, 52 °C for 30 s, 72 °C for 25 s to produce double-strand DNA (dsDNA). Next, the T7 RNA transcription kit was used to produce the RNA target with the dsDNA as the template. Finally, the dsDNA was degraded by DNase I at 37 °C for 1 h. And then the transcriptional products were purified by MiRcute miRNA Isolation Kit (DP501, Tiangen) and stored at −20 °C. And 2% Agarose gel was used to testify the results, shown in Fig. S2 (Supporting information).

2.3. Synthesis of crRNA

CrRNA was synthesized and purified according to previously reported methods [38]. The principle and results of crRNA were shown in Fig. S3 and Fig. S4 (Supporting information).

2.4. Construction of the biosensor

The reaction reagent of the whole biosensor was divided into reagent A and B. Reagent A was responsible for the RT-RPA reaction, containing 5.9 μL Resuspended RPA solution, 0.5 μL 10 μM Orf1ab-RPA-Forward or S-RPA-Forward, 0.5 μL 10 μM Orf1ab-RPA-Reverse or S-RPA-Reverse, 1

μL ProtoScript® II Reverse Transcriptase, 0.4 μL RNase-Free H_2O, 2.5 μL MgAc. Reagent B consisted of 2 μL NEB Buffer 2.1, 8.6 μL RNase-Free H_2O, 2 μL 1 μM LwCas13a, 1 μL 2 μM S-crRNA or Orf1ab-crRNA, 1 μL 10 μM RNA probes, 1 μL RNase inhibitor, 0.6 μL T7 polymerase, 0.8 μL Ribonucleotide solution and 1 μL MgAc (280 mM), which was responsible for the transcription and the CRISPR/Cas13a system. One microliter sample was added to reagent A and incubated at 37 °C for 10 min. Then, reagent B was added to reagent A and incubated at 37 °C for 20 min.

2.5. Determination of SARS-CoV-2 by lateral flow strip

After the reaction of RT-RPA and CRISPR/Cas13a, 80 μL double distilled water was added for detection of the lateral flow strip. A lateral flow strip was inserted into the reaction solution for 2 min. What was noteworthy was that positive samples should show two lines, while negative samples should show only a C line. Moreover, each sample needed to be checked whether the S and Orf1ab genes all appear in two lines, which can increase the detection accuracy of SARS-CoV-2.

2.6. Design and development of APHF-analyzer

To facilitate rapid and accurate detection of SARS-CoV-2, we developed an automatic, portable, and high-throughput fluorescence analyzer (APHF-analyzer). It was mainly composed of five parts: liquid circuit detection subsystem, optical signal detection subsystem, mechanical transmission subsystem, circuit control subsystem, and temperature-controlled subsystem. The 3D-printed microfluidic chip, made by polylactic acid (PLA), was served as the basic unit of the liquid circuit detection system for detection. The parameters of the microfluidic chip were in Table S2 (Supporting information). The optical sensing subsystem was divided into two parts: the excitation light source module including a cost-effective white light-emitting diode (LED) and the laser with wavelengths of 488 nm, and a micro-spectrometer purchased from Ocean Insight Inc. (Florida, USA) with necessary optical support structure design for capturing the emission spectrum. The circuit control subsystem integrated a single-chip Microcontroller (STM32F103 MCU, designed by STMicroelectronics company) and its peripheral circuits. This subsystem not only received commands from the host computer embedded ARM11 (designed by Texas Instruments company) to control the peripherally functional modules but also was responsible for the resources distribution to ensure the operation of the entire system smoothly. And all actions were controlled by the mechanical transmission system. The mechanical transmission subsystem consisted of the motor, guide rail, positioning device, and displacement device. Dual drive guide rail (upper, lower) was designed to meet the requirements of positioning, multi-displacement, and low detection error. There were two types available switch of excitation light source in the upper tracks, and the lower guide rail can realize the switch of each working position including initializing working position, placing chip working position, detecting the working position, and pop-up chip position. In addition, a K-type thermocouple was selected as the temperature sensor and saw Supporting Information for details.

The APHF-analyzer was employed as a powerful instrument to detect SARS-CoV-2. The sample and reagent A were added into storage chamber 1, and reagent B was added in chamber 2 of the microfluidic chip, respectively. After RT-RPA reaction in chamber 1, the liquid entered chamber 3 mixing with reagent B via the motor rotating to carry out the transcription and the CRISPR/Cas13a reaction. Finally, the optical fiber spectrometer recognized and recorded the fluorescence signal under the laser with the excitation of 488 nm.

2.7. Determination of SARS-CoV-2 in real sample

The nucleic acids samples were provided by the Chongqing University Cancer Hospital, 2 μL of which were carried out RT-RPA, transcription, and the CRISPR/Cas13a detection. Finally, the signal was performed by APHF-analyzer and lateral flow strip.

3. Results and discussion

3.1. Principle of the biosensor to detect SARS-CoV-2

Scheme 1 illustrates the principle of CRISPR/Cas13a-based biosensor coupled with RT-RPA for SARS-CoV-2 assay. Firstly, the S gene and Orf1ab gene as targets, trigger the process of reverse transcription recombinase polymerase amplification (RT-RPA) and transcription, producing a large number of RNA targets. Then, the *trans*-cleavage activity of Cas13a is activated via recognizing and combining the transcripts by complementation between the transcripts and crRNAs, meaning that large amounts of non-specific RNA probes can be arbitrarily cut. This is a specific signal amplification of the biosensor. Among them, transcription, as the second signal amplification technology of the biosensor based RT-RPA, is a method to prevent pollution. Since the amplification efficiency of RPA is very high, causing aerosol pollution and increasing the risk of background signal for subsequent detection. Through transcription, DNA products are turned into RNA, which is recognized by CRISPR/Cas13a, which can further improve specificity and avoid contamination. Hence, in contrast to the method based CRISPR-Cas12a combined with RT-RPA, Cas13a with transcription is a good method to eliminate false positives and improves accuracy. As a result, with three signal amplification, the biosensor could detect low concentrations of SARS-CoV-2 in a short time.

To achieve visual and point of care detection, we built the biosensor on a lateral flow strip. FAM and biotin are attached to both ends of the RNA probes. The probes attached the FAM can bind to gold nanoparticles with an anti-FAM antibody. As the liquid flows, the streptavidin on the C line captures the probe with the biotin. As a consequence, the complete RNA probes are intercepted on the C line. While, Cas13a is activated to cleave the RNA probes in the presence of targets. The severed probes with FAM will bind with gold nanoparticles with anti-FAM antibody, which are intercepted by the capture antibody of the T line due to the fact that the severed probes without biotin cannot be intercepted by the C line. Hence, the lateral flow strip will show only a T line or two lines when the RNA target is present. And there is only a C line in the case of no target.

Moreover, aiming to achieve high throughput and rapid detection in response to the COVID-19 outbreak, an APHF-analyzer [39] with a microfluidic chip was developed to accurately detect SARS-CoV-2. Its components are described in Section 2.6. The sample is added to a microfluidic chip where all the reactions take place. And the microfluidic chip is placed in the APHF-analyzer to quickly collect signals. By exquisitely designed, a chip can simultaneously detect two samples, which saves time and cost. What's more, the airtightness of the chip is excellent, which can reduce cross pollution and aerosol pollution that are the most common and serious problems in SARS-CoV-2 detection. And chips can be mass produced due to the fact that they are easy to operate and cost-effective, which can greatly reduce the pressure on the medical staff. APHF-analyzer realized automated and high-throughput detection through an accurate temperature control system, liquid circuit detection subsystem, optical signal detection subsystem, mechanical transmission subsystem, and circuit control subsystem. As a result, APHF-analyzer with the microfluidic chip would serve as a fundamental detecting tool.

3.2. The development of the APHF-analyzer

The ability to high throughput detect for SARS-CoV-2 would serve as a fundamental element in combating the outbreak. We developed an APHF-analyzer for rapid and sensitive detection of SARS-CoV-2. The system detected SARS-CoV-2 in the liquid phase. Fig. 1(a) exhibited a physical picture of the APHF-analyzer. It consisted of the liquid circuit

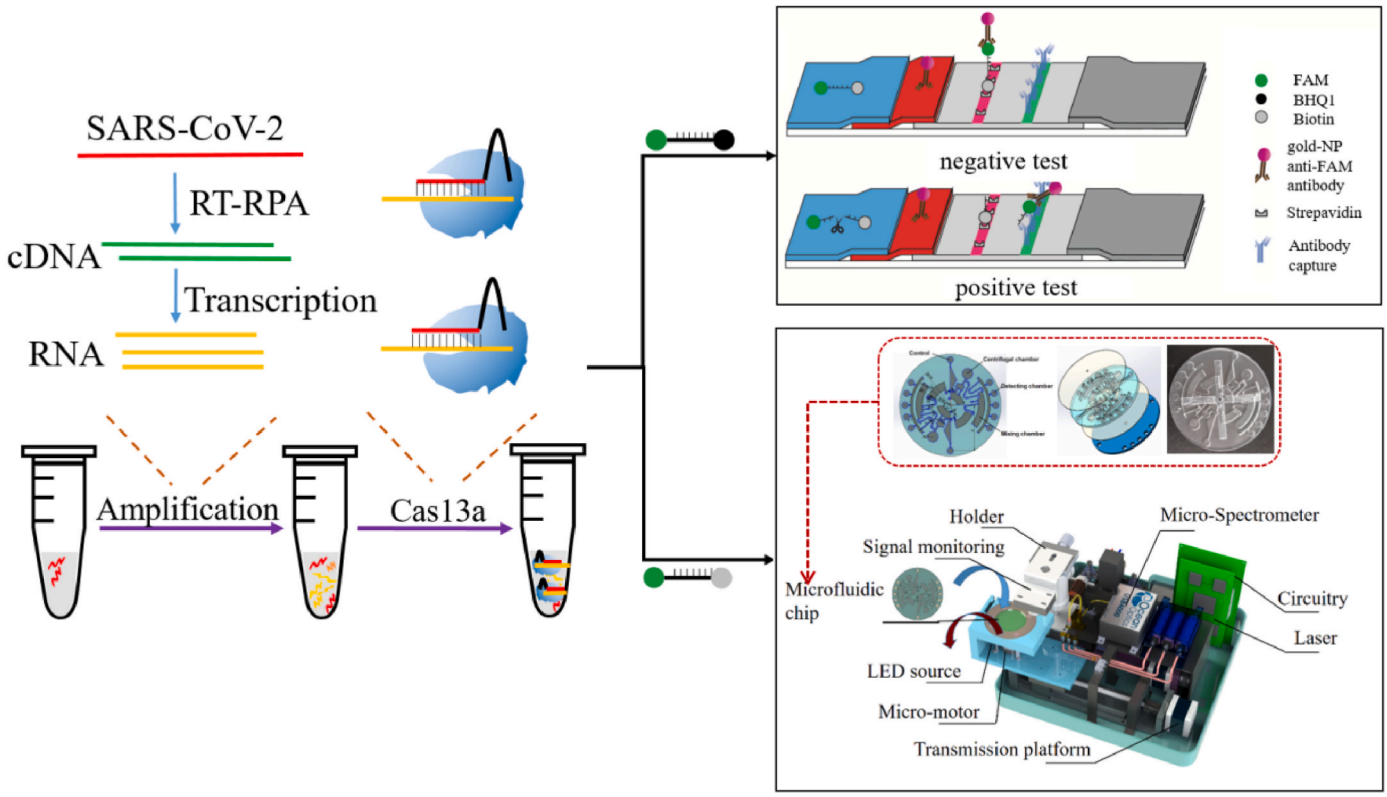

Scheme 1. Schematic illustration of the detecting SARS-CoV-2 strategy combined CRISPR/Cas13a with RPA by LS-55 spectrophoto fluorometer, lateral flow strip, and APHF-analyzer.

detection subsystem, optical signal detection subsystem, mechanical transmission subsystem, circuit control subsystem, and temperature-controlled subsystem. The microfluidic chip can be embedded in the disk reaction chamber and can be rotated freely after receiving the transmission instruction. After accomplishing all reactions by the precise temperature control system and mechanical transmission subsystem, the APHF-analyzer can acquire fluorescence signals through the optical signal detector and sensor array optical signal responding to monitor signals before and after the reaction. And it outputted the date with the aid of subsequent signal processing and feature extraction algorithm. It realized automatic, micro-trace, high-throughput, and accurate detection samples through the linkage and coordination among subsystems. As shown in Fig. 1(b), the microfluidic chip was made up of four layers. Among them, the first layer and the third layer were made by medically grade Polypropylene film (PP film) for optical detection. The second layer included a parallel detection chamber, control chamber, analytically mixed chamber, centrifugal chamber, and valve and microchannel structure. The fourth layer was connected to the fixed layer to facilitate the installation of the chip on the rotating shaft of the gas chamber. All the processes of the biosensor take place on the chip, which avoids aerosol contamination and makes the detection more accurate and easy to operate. And its symmetrical detection areas can detect two samples at the same time.

3.2.1. *Performance of the APHF-analyzer for SARS-CoV-2 detection*

In the presence of SARS-CoV-2, the amplified process of RT-RPA and transcription and *trans*-cleavage of CRISPR/Cas13a could be taken place, resulting in large amounts of fluorescence signal. As described in Fig. 2(a), the fluorescence intensity of the S gene was collected by the APHF-analyzer. The collected spectral signals were smoothed to obtain smooth fluorescence signals with good symmetry in Fig. 2(b). Obviously, the fluorescence intensity of the test group was significantly higher than that of the control group. In the presence of the S gene, the chip displayed green fluorescence under laser irradiation in Fig. 2(c). In contrast, the chip was just blue, which was the color of the light itself without targets (Fig. 2(d)). These indicated that the APHF-analyzer has great potential to detect SARS-CoV-2.

3.2.2. *The performance of the APHF-analyzer*

To verify the performance of the APHF-analyzer, different concentrations of the S gene and Orf1ab gene were detected by the APHF-analyzer. As shown in Fig. 3(b) and (e), after smoothing, data showed that fluorescence intensity gradually increased with the increase of concentration of the S gene and Orf1ab gene. There was a good linear relation between Δ F (Δ F refers to the difference of fluorescence intensity between the test and control group) and the logarithmic of the concentration of the S gene from 10 fM to 10 nM. The linear equation was $\Delta F = 298.2 \times \lg C - 233.6$ ($R^2 = 0.9914$), and the LOD was 0.68 fM according to the 3σ rule. In addition, the linear equation between fluorescence intensity and the logarithm of the Orf1ab gene concentration was $\Delta F = 302.08 \times \lg C - 159.7$ ($R^2 = 0.9923$), with LOD as 4.16 fM. This demonstrated that the APHF-analyzer can highly sensitively detect SARS-CoV-2.

In addition, to demonstrate the capability of the APHF-analyzer, a comparison was made with a commercial LS-55 spectrophoto fluorometer. As shown in Fig. 4(a), as the concentration of the S gene increased from 20 fM to 2 nM, the fluorescence intensity increased continuously. This indicated that the increase of target can generate more amplification products and activate more Cas13a to shear RNA probes to generate signals. As Fig. 4(b) displayed a good linear dependence between the Δ F and the logarithm of the concentration of the S gene from 20 fM to 200 pM with the linear regression equation of $\Delta F = -280.434 + 289.694 \times \lg C$ ($R^2 = 0.9949$). According to the 3σ rule, the LOD was as low as 9.2 fM. Similarly, different concentrations of the Orf1ab gene were detected. It was found that the fluorescence intensity increased with elevated concentration from 20 fM to 2 nM in Fig. 4(c). There was a linear

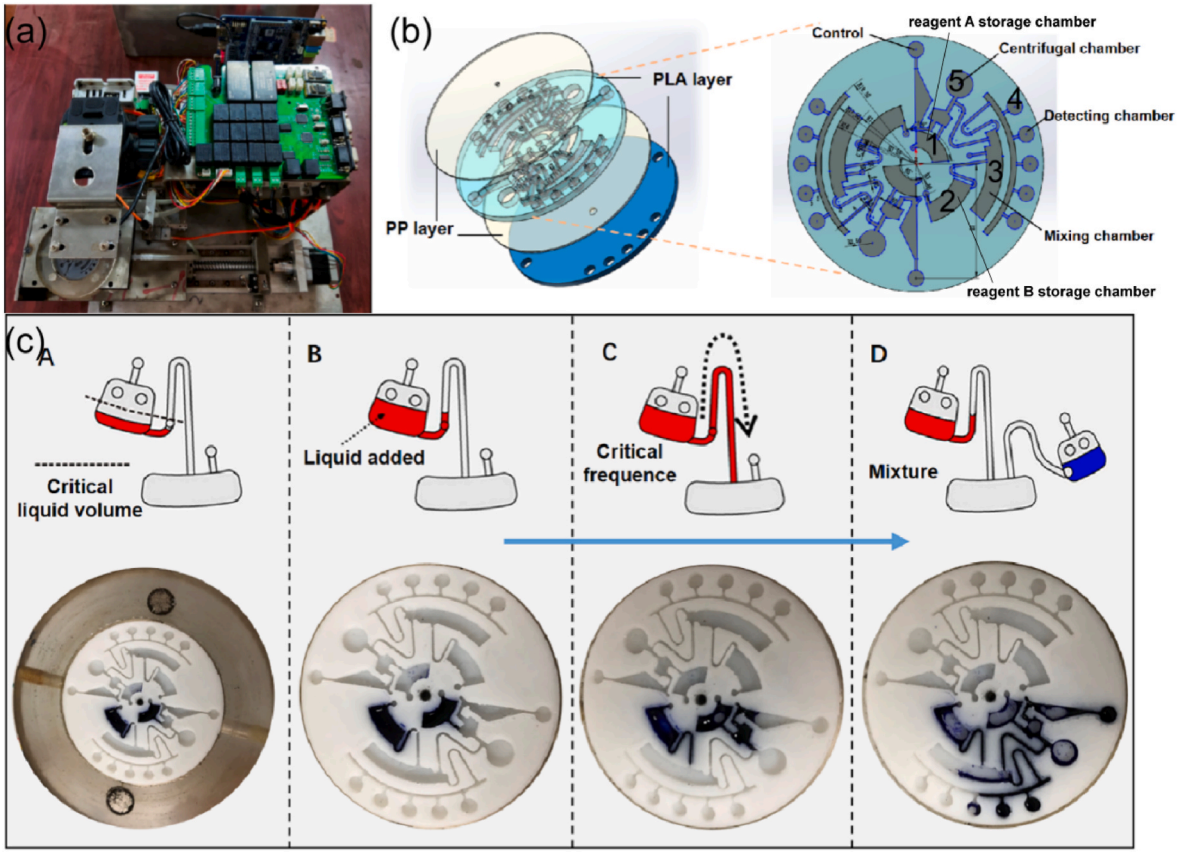

Fig. 1. Structure of the APHF-analyzer. (a) Showed a physical picture of the APHF-analyzer. (b) Depicted view of the device showing the four layers: top and third disks are PP layer; the second disk with 12 sample holes and channel structures; the bottom layer for the installation. (c) The actual test results of dye.

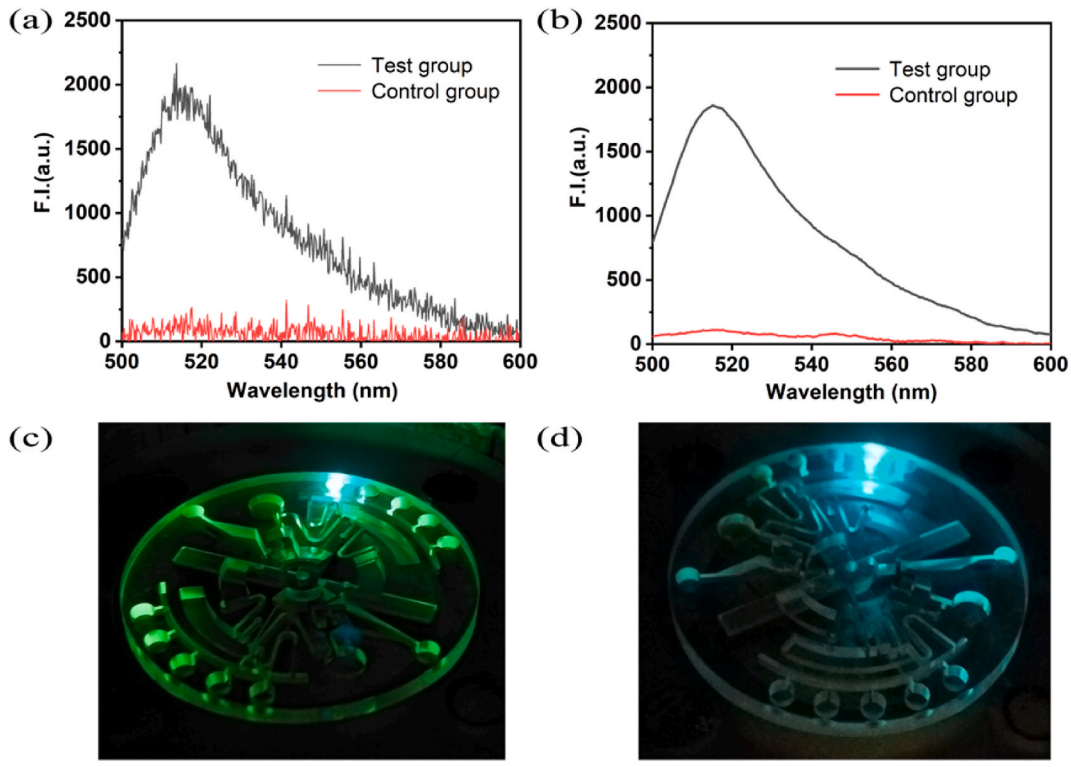

Fig. 2. S gene of SARS-CoV-2 detected by the APHF-analyzer. (a) Showed the collected spectral signals of the test and the control group. (b) Described the signals after smoothed. (c) and (d) showed the chip images of the test and control groups.

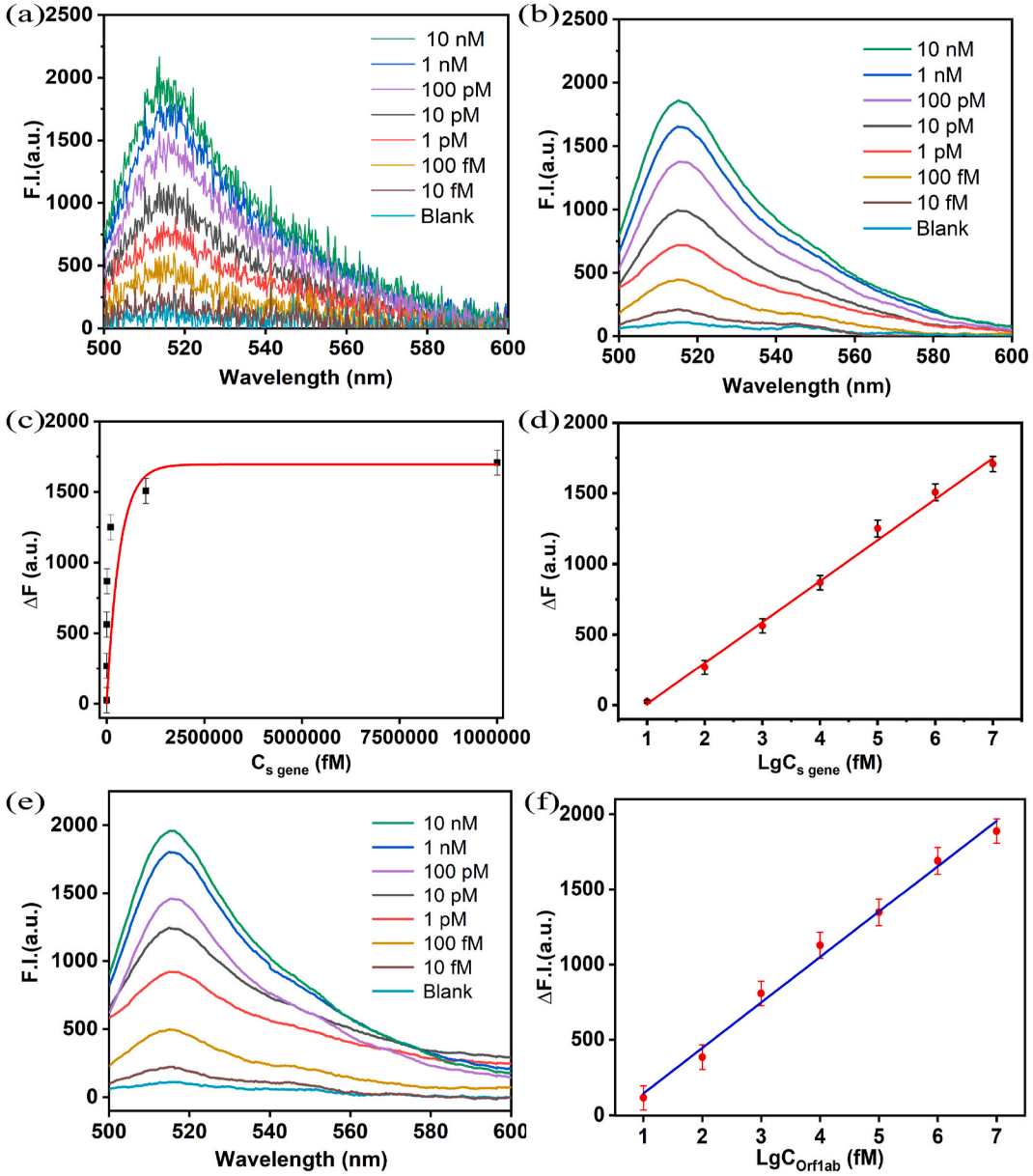

Fig. 3. Different concentrations of the S gene and Orf1ab gene of SARS-CoV-2 were detected by the APHF-analyzer. (a)The fluorescence intensity corresponding to the S gene with different concentrations from 10 fM to 10 nM. (b) The signals after smoothed. (c) The relation between Δ F and the concentration of the S gene from 10 fM to 10 nM. (d)The linear relation between Δ F and the logarithmic of the concentration of the S gene from 10 fM to 10 nM. (e) The fluorescence intensity corresponding to the Orf1ab gene with different concentrations from 10 fM to 10 nM after smoothed. (f) The linear relation between Δ F and the logarithmic of the concentration of the Orf1ab gene from 10 fM to 10 nM.

relation between Δ F and logarithm of the concentration of the Orf1ab gene from 20 fM to 2 nM in Fig. 4(d). The linear equation was $\Delta F = 144.7 \times \lg C\text{-}177.0$, ($R^2 = 0.9829$), and the LOD was as low as 17.25 fM.

The above results indicated that the APHF-analyzer has higher sensitivity than the commercial LS-55 spectrophoto fluorometer, which proved that the APHF-analyzer was on a par with a large fluorescence spectrophotometer. In addition, with the use of a microfluidic chip, the APHF-analyzer achieved high throughput and automatic detection, which was of great help to the detection of SARS-CoV-2. Therefore, the APHF-analyzer is a promising tool for high-throughput, sensitive, and automated detection of SARS-CoV-2. In contrast to other methods utilizing the CRISPR/Cas system in Table S3, the APHF-analyzer coupled with the biosensor has strong sensitivity in a short detection time. This gives the credit to the sensitivity of the instrument and triple signal amplification of the biosensor, RT-RPA, transcription, and the strong *trans*-cutting activity of Cas13a.

3.2.3. *The specificity, reproducibility, and repeatability of the APHF-analyzer*

Specificity, Reproducibility, and repeatability are important indicators of a sensor. Fig. 5(a) described nucleic acid detection of different viruses with the same concentration of 100 pM by the APHF-analyzer, such as SARS-CoV-2, SARS-CoV, Hs-RPP30, MERS-CoV. It was found that the fluorescence intensity of SARS-CoV-2 was significantly higher than that of other viruses, indicating that the APHF-analyzer combined with RPA and CRISPR/Cas13a had a strong specificity for the detection of the S gene and Orf1ab gene. Fig. 5(b) showed five experiments with 1 pM S gene were used to test the reproducibility of APHF-analyzer with a relative standard deviation (RSD) of 3.42%. And Fig. 5(c) depicted good repeatability of the APHF-analyzer. Those

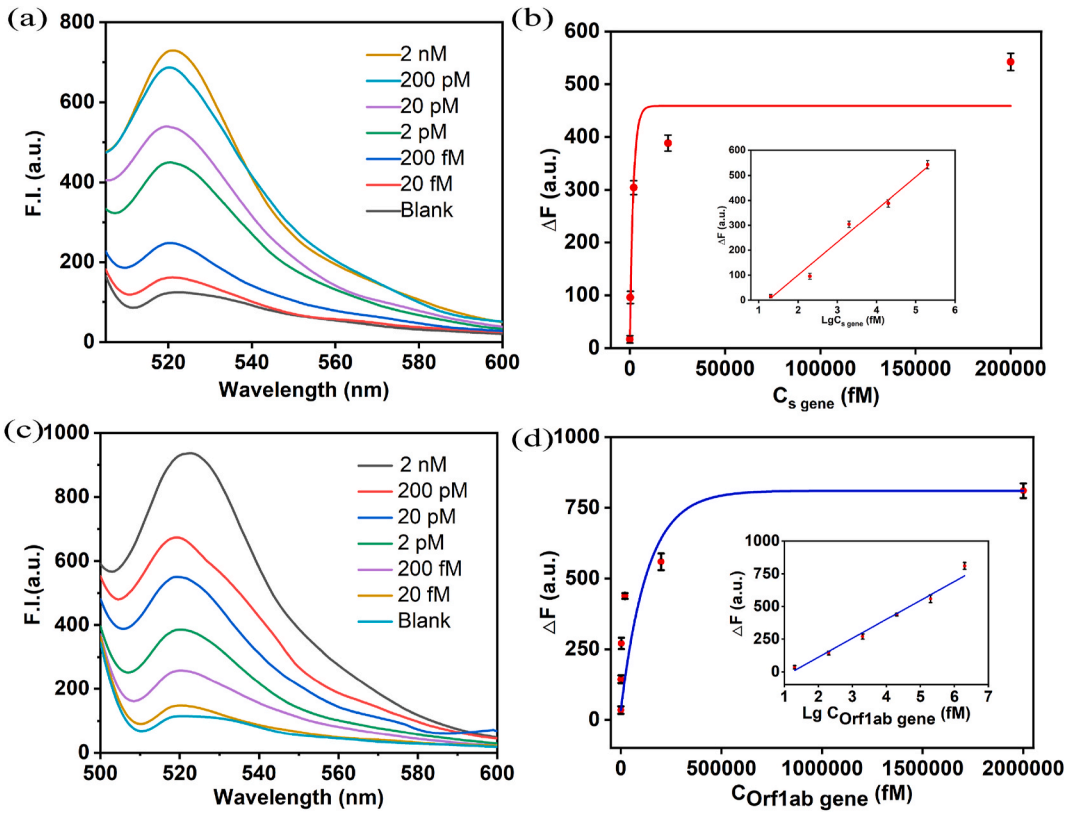

Fig. 4. The fluorescence intensity of the biosensor for various concentrations of the S and Orf1ab genes. (a) Thefluorescence intensity of the S gene at different concentrations from 20 fM to 2 nM. (b) The relationship between Δ F and logarithm of the concentration of the S gene from 20 fM to 200 pM. (c) The fluorescence intensity of the Orf1ab gene with different concentrations from 20 fM to 2 nM. (d) The relationship between Δ F and logarithm of the concentration of the Orf1ab gene from 20 fM to 2 nM.

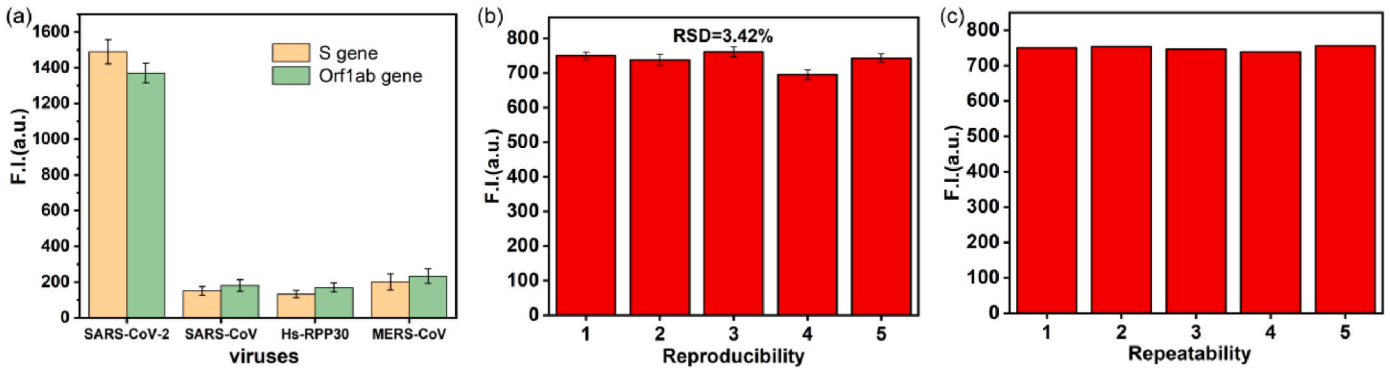

Fig. 5. Specificity, Reproducibility and repeatability of the APHF-analyzer with 1 pM S gene of SARS-CoV-2.

indicated that the APHF-analyzer based RT-RPA and CRISPR/Cas13a had excellent reproducibility and repeatability for detecting SARS-CoV-2.

3.3. The performance of lateral flow strip to detect SARS-CoV-2

Fig. 6(a) depicted that the different concentrations of the S gene were detected by the lateral flow strip. With the increase of concentration, the T line became more and more obvious, while the C line band became weaker and weaker. It illustrated that more RNA probes were cut as the S gene increased. And Fig. 6(a) showed a relationship between the brightness of the T line and the concentration of the S gene from 200 aM to 20 pM. A surprise was that the LOD of lateral flow strip to S gene was as low as 2 fM. In the same way, the lateral flow strip was used to detect the Orf1ab gene with different concentrations. Fig. 6(b) showed as the concentration of the Orf1ab gene increased, the brightness of the T line increased, while the brightness of the C line decreased. The LOD of the lateral flow strip for the Orf1ab gene was as low as 20 fM.

3.4. Detection of SARS-CoV-2 in the actual sample

Nucleic acids were extracted from pharyngeal swabs of patients by medical staff according to the standard way. The nucleic acid was detected by the biosensor combined CRISPR/Cas13a with RT-RPA. The results of the S gene and Orf1ab gene detection were shown in Fig. 7(a) and (b). It was obvious that the fluorescence intensity of the positive sample was significantly higher than that of the negative sample. And Fig. 7(c) and (d) demonstrated the results of the S gene and Orf1ab gene

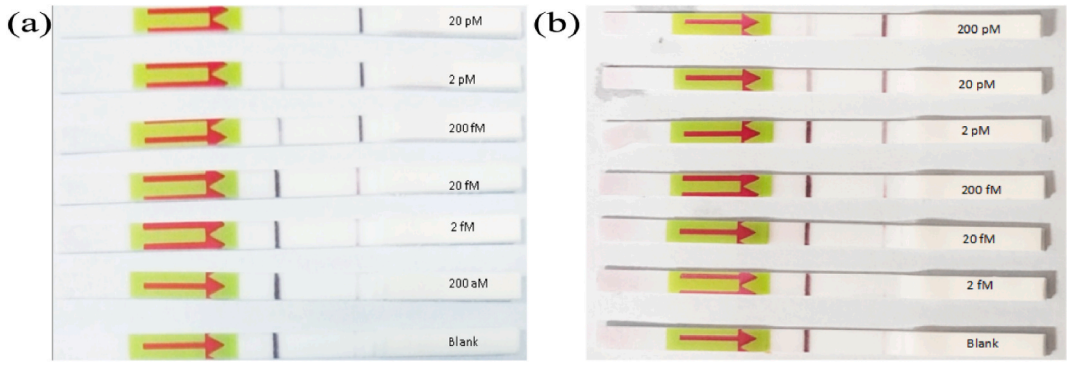

Fig. 6. (a) The sensitivity detection of SARS-CoV-2 biosensor for different concentrations of S gene from 200 aM to 20 pM by lateral flow strip. (b) The lateral flow strip assay with different concentrations of the Orf1ab gene from 2 fM to 200 pM.

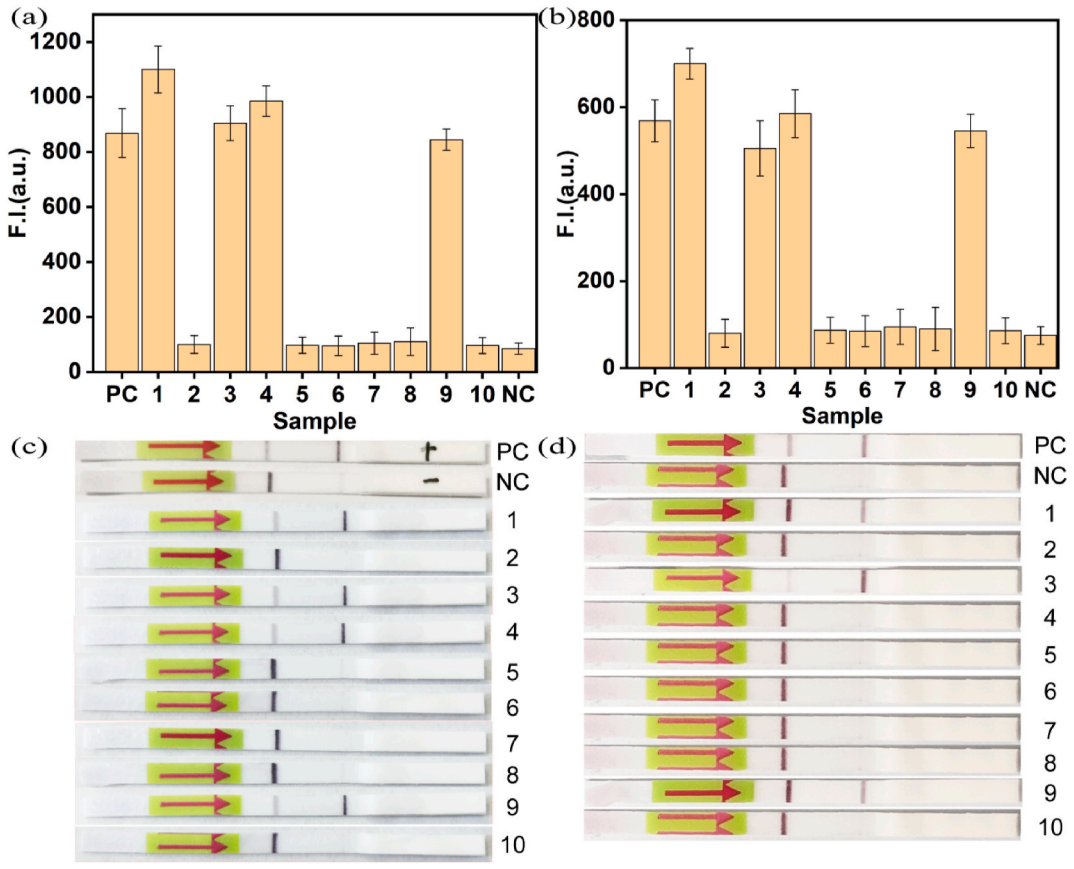

Fig. 7. SARS-CoV-2 detection of actual samples. (a) and (b) The fluorescence intensity of samples to the S gene and Orf1ab gene, respectively. (c) and (d) The results of the S gene and Orf1ab gene in actual samples tested by the lateral flow strip.

detected by the lateral flow strip, respectively. The positive sample had an obvious T line, while the negative sample had only a C line. The above results expounded that the APHF-analyzer and lateral flow strip based CRISPR/Cas13a with RT-RPA can accurately and quickly distinguish between positive samples and negative samples.

4. Conclusions

SARS-CoV-2 has been wreaking havoc around the world since December 2019, bringing great damage to the world. SARS-CoV-2 detection is a key in the process of quickly ending the pandemic. We developed a biosensor based on CRISPR/Cas13a with RPA, which realized sensitive and specific detection of SARS-CoV-2 in 30 min. Taking full advantage of the biosensor, we used the lateral flow strip to detect the S gene and Orf1ab gene with the actual limit of detection of 2 fM and 20 fM. By lateral flow strip, the biosensor achieved visual detection, facilitated self-test at the grassroots level and reduced the pressure on hospitals. What's more, in order to realize high-throughput and automatic detection, we developed the APHF-analyzer to facilitate rapid and sensitive detection of SARS-CoV-2. The LOD of S gene and Orf1ab gene were as low as 0.68 fM and 4.16 fM, which is more sensitive than the large commercial fluorescence spectrophotometer. The APHF-analyzer is very beneficial for testing large numbers of samples because of the short detection time, high throughput and accurate performance. As a consequence, the APHF-analyzer and the lateral flow strip based on biosensor can satisfy the requirement of sensitive, fast, high-throughput,

and on-site detection of SARS-CoV-2, and we believe that the lateral flow strip and APHF-analyzer will make a huge contribution to the world's fight against COVID-19.

Declaration of competing interest

The authors declare that they have no known competing financial interests or personal relationships that could have appeared to influence the work reported in this paper.

Acknowledgments

This work was supported by the Fundamental Research Funds for the Central Universities (2020CDJYGRH-YJ06), Chongqing Graduate Tutor Team Construction Project, Analytical and Testing Center of Chongqing University, and the sharing fund of Chongqing University's large equipment.

Appendix A. Supplementary data

Supplementary data to this article can be found online at https://doi.org/10.1016/j.talanta.2022.123594.

References

[1] C.Y. Yang, J. Wang, Transmission rates and environmental reservoirs for COVID-19-a modeling study, J. Biol. Dynam. 15 (1) (2021) 86–108.
[2] Q. Wang, T. Yang, Y. Wang, Reduced treatment sensitivity of SARS-CoV-2 after multigenerational human-to-human transmission, Front. Phys.-Lausanne 8 (2020).
[3] W. Ahmed, B. Tscharke, P.M. Bertsch, K. Bibby, A. Bivins, P. Choi, L. Clarke, J. Dwyer, J. Edson, T.M.H. Nguyen, J.W. O'Brien, S.L. Simpson, P. Sherman, K. V. Thomas, R. Verhagen, J.L. Zaugg, J.F. Mueller, SARS-CoV-2 RNA monitoring in wastewater as a potential early warning system for COVID-19 transmission in the community: a temporal case study, Sci. Total Environ. (2021) 761.
[4] K. Kitamura, K. Sadamasu, M. Muramatsu, H. Yoshida, Efficient detection of SARS-CoV-2 RNA in the solid fraction of wastewater, Sci. Total Environ. 763 (2021).
[5] W.L. Chen, Y. Lan, X.Z. Yuan, X.L. Deng, Y.P. Li, X.L. Cai, L.Y. Li, R.Y. He, Y.Z. Tan, X.Z. Deng, M. Gao, G.F. Tang, L.Z. Zhao, J.L. Wang, Q.H. Fan, C.Y. Wen, Y.W. Tong, Y.B. Tang, F.Y. Hu, F. Li, X.P. Tang, Detectable 2019-nCoV viral RNA in blood is a strong indicator for the further clinical severity, Emerg. Microb. Infect. 9 (1) (2020) 469–473.
[6] Z.H. Chen, Z.G. Zhang, X.M. Zhai, Y.Y. Li, L. Lin, H. Zhao, L. Bian, P. Li, L. Yu, Y. S. Wu, G.F. Lin, Rapid and sensitive detection of anti-SARS-CoV-2 IgG, using lanthanide-doped nanoparticles-based lateral flow immunoassay, Anal. Chem. 92 (10) (2020) 7226–7231.
[7] H.Y. Chung, M.J. Jian, C.K. Chang, J.C. Lin, K.M. Yeh, C.W. Chen, S.K. Chiu, Y. H. Wang, S.J. Liao, S.Y. Li, S.S. Hsieh, S.H. Tsai, C.L. Perng, J.R. Yang, M.T. Liu, F. Y. Chang, H.S. Shang, Novel dual multiplex real-time RT-PCR assays for the rapid detection of SARS-CoV-2, influenza A/B, and respiratory syncytial virus using the BD MAX open system, Emerg. Microb. Infect. 10 (1) (2021) 161–166.
[8] S. Cavalera, B. Colitti, S. Rosati, G. Ferrara, L. Bertolotti, C. Nogarol, C. Guiotto, C. Cagnazzo, M. Denina, F. Fagioli, F. Di Nardo, M. Chiarello, C. Baggiani, L. Anfossi, A multi-target lateral flow immunoassay enabling the specific and sensitive detection of total antibodies to SARS COV-2, Talanta (2021) 223.
[9] A. Roda, S. Cavalera, F. Di Nardo, D. Calabria, S. Rosati, P. Simoni, B. Colitti, C. Baggiani, M. Roda, L. Anfossi, Dual lateral flow optical/chemiluminescence immunosensors for the rapid detection of salivary and serum IgA in patients with COVID-19 disease, Biosens. Bioelectron. 172 (2021).
[10] H.X. Liu, K.C. Shi, W.C. Sun, J. Zhao, Y.W. Yin, H.B. Si, S.J. Qu, W.J. Lu, Development a multiplex RT-PCR assay for simultaneous detection of African swine fever virus, classical swine fever virus and atypical porcine pestivirus, J. Virol Methods 287 (2021).
[11] C.L. Perng, M.J. Jian, C.K. Chang, J.C. Lin, K.M. Yeh, C.W. Chen, S.K. Chiu, H. Y. Chung, Y.H. Wang, S.J. Liao, S.Y. Li, S.S. Hsieh, S.H. Tsai, F.Y. Chang, H. S. Shang, Novel rapid identification of severe acute respiratory syndrome coronavirus 2 (SARS-CoV-2) by real-time RT-PCR using BD max open system in Taiwan, PeerJ 8 (2020).
[12] A.B. Gussow, N. Auslander, G. Faure, Y.I. Wolf, E.V. Koonin, Genomic determinants of pathogenicity in SARS-CoV-2 and other human coronaviruses, Proc. Natl. Acad. Sci. Unit. States Am. 117 (26) (2020) 202008176.
[13] O. Belmehdi, M. Hakkour, N. El Omani, A. Balahbib, F.E. Guaouguaou, T. Benali, A. El Baaboua, M. Lahmoud, N. Elmenyiy, A. Bouyahya, Molecular structure, pathophysiology, and diagnosis of COVID-19, Biointerface Res App 11 (3) (2021) 10215–10237.
[14] M.S.R. A, M.N.H.A. B, M.R.I. A, I.I. A, I.D.M. A, M.M.R. A, M.S. A, M.A.H. A, Mutational Insights into the Envelope Protein of SARS-CoV-2 - ScienceDirect, Gene Reports. 22.
[15] Z.Q. Zhou, Y.Z. Zhang, M.Z. Guo, K.L. Huang, W.T. Xu, Ultrasensitive magnetic DNAzyme-copper nanoclusters fluorescent biosensor with triple amplification for the visual detection of E. coli O157: H7, Biosens. Bioelectron. 167 (2020).
[16] R. Wang, C.Y. Qian, Y.A. Pang, M.M. Li, Y. Yang, H.J. Ma, M.Y. Zhao, F. Qian, H. Yu, Z.P. Liu, T. Ni, Y. Zheng, Y.M. Wang, opvCRISPR: one-pot visual RT-LAMP-CRISPR platform for SARS-cov-2 detection, Biosens. Bioelectron. 172 (2021).
[17] Y.J. Chen, Y. Shi, Y. Chen, Z. Yang, H. Wu, Z.H. Zhou, J. Li, J.F. Ping, L.P. He, H. Shen, Z.X. Chen, J. Wu, Y.S. Yu, Y.J. Zhang, H. Chen, Contamination-free visual detection of SARS-CoV-2 with CRISPR/Cas12a: a promising method in the point-of-care detection, Biosens. Bioelectron. 169 (2020).
[18] X.K. Wang, X.D. Wang, C. Shi, C.P. Ma, L.X. Chen, Highly sensitive visual detection of nucleic acid based on a universal strand exchange amplification coupled with lateral flow assay strip, Talanta 216 (2020).
[19] A. Scharf, C. Lang, M. Fischer, Genetic authentication: differentiation of fine and bulk cocoa (Theobroma cacao L.) by a new CRISPR/Cas9-based in vitro method, Food Control 114 (2020).
[20] K. Pardee, A.A. Green, M.K. Takahashi, D. Braff, G. Lambert, J.W. Lee, T. Ferrante, D. Ma, N. Donghia, M. Fan, N.M. Daringer, I. Bosch, D.M. Dudley, D.H. O'Connor, L. Gehrke, J.J. Collins, Rapid, low-cost detection of zika virus using programmable biomolecular components, Cell 165 (5) (2016) 1255–1266.
[21] Y.M. Zhang, Y. Zhang, K.B. Xie, Evaluation of CRISPR/Cas12a-based DNA detection for fast pathogen diagnosis and GMO test in rice, Mol. Breed. 40 (1) (2020).
[22] M.N. Esbin, O.N. Whitney, S.S. Chong, A. Maurer, X. Darzacq, R. Tjian, Overcoming the bottleneck to widespread testing: a rapid review of nucleic acid testing approaches for COVID-19 detection, RNA 26 (7) (2020) 771–783.
[23] J.Y. Wang, C.Z. Zhang, B. Feng, The rapidly advancing Class 2 CRISPR-Cas technologies: a customizable toolbox for molecular manipulations, J. Cell Mol. Med. 24 (6) (2020) 3256–3270.
[24] S.Y. Li, Q.X. Cheng, J.M. Wang, X.Y. Li, Z.L. Zhang, S. Gao, R.B. Cao, G.P. Zhao, J. Wang, CRISPR-Cas12a-assisted nucleic acid detection, Cell Discov. 4 (2018).
[25] Q. He, D.M. Yu, M.D. Bao, G. Korensky, J.H. Chen, M.Y. Shin, J.W. Kim, M. Park, P. W. Qin, K. Du, High-throughput and all-solution phase African Swine Fever Virus (ASFV) detection using CRISPR-Cas12a and fluorescence based point-of-care system, Biosens. Bioelectron. 154 (2020).
[26] H. Khan, A. Khan, Y.F. Liu, S. Wang, S. Bibi, H.P. Xu, Y. Liu, S. Durrani, L. Jin, N. Y. He, T. Xiong, CRISPR-Cas13a mediated nanosystem for attomolar detection of canine parvovirus type 2, Chin. Chem. Lett. 30 (12) (2019) 2201–2204.
[27] R. Bruch, J. Baaske, C. Chatelle, M. Meirich, S. Madlener, W. Weber, C. Dincer, G. A. Urban, CRISPR/Cas13a-Powered electrochemical microfluidic biosensor for nucleic acid amplification-free miRNA diagnostics, Adv. Mater. 31 (51) (2019).
[28] L.B. Harrington, D. Burstein, J.S. Chen, D. Paez-Espino, E. Ma, I.P. Witte, J. C. Cofsky, N.C. Kyrpides, J.F. Banfield, J.A. Doudna, Programmed DNA destruction by miniature CRISPR-Cas14 enzymes, Science 362 (6416) (2018) 839(. -+).
[29] J.P. Broughton, X.D. Deng, G.X. Yu, C.L. Fasching, V. Servellita, J. Singh, X. Miao, J.A. Streithorst, A. Granados, A. Sotomayor-Gonzalez, K. Zorn, A. Gopez, E. Hsu, W. Gu, S. Miller, C.Y. Pan, H. Guevara, D.A. Wadford, J.S. Chen, C.Y. Chiu, CRISPR-Cas12-based detection of SARS-CoV-2, Nat. Biotechnol. 38 (7) (2020) 870 (. -+).
[30] L. Guo, X.H. Sun, X.G. Wang, C. Liang, H.P. Jiang, Q.Q. Gao, M.Y. Dai, B. Qu, S. Fang, Y.H. Mao, Y.C. Chen, G.H. Feng, Q. Gu, R.R. Wang, Q. Zhou, W. Li, SARS-CoV-2 detection with CRISPR diagnostics, Cell Discov. 6 (1) (2020).
[31] Y. Sha, R. Huang, M.Q. Huang, H.H. Yue, Y.Y. Shan, J.M. Hu, D. Xing, Cascade CRISPR/cas enables amplification-free microRNA sensing with fM-sensitivity and single-base-specificity, Chem. Commun. 57 (2) (2021) 247–250.
[32] R. Aman, A. Mahas, M. Mahfouz, Nucleic acid detection using CRISPR/cas biosensing technologies, ACS Synth. Biol. 9 (6) (2020) 1226–1233.
[33] M.Q. Huang, R. Huang, H.H. Yue, Y.Y. Shan, D. Xing, Ultrasensitive and high-specific microRNA detection using hyper-branching rolling circle amplified CRISPR/Cas13a biosensor, Sensor. Actuator. B Chem. 325 (2020).
[34] R. Wang, C.R. Simoneau, J. Kulsuptrakul, M. Bouhaddou, K.A. Travisano, J. M. Hayashi, J. Carlson-Stevermer, J.R. Zengel, C.M. Richards, P. Fozouni, J. Oki, L. Rodriguez, B. Joehnk, K. Walcott, K. Holden, A. Sil, J.E. Carette, N.J. Krogan, M. Ott, A.S. Puschnik, Genetic screens identify host factors for SARS-CoV-2 and common cold coronaviruses, Cell 184 (1) (2021) 106–+.
[35] P. Fozouni, S.M. Son, M.D.D. Derby, G.J. Knott, C.N. Gray, M.V. D'Ambrosio, C. Y. Zhao, N.A. Switz, G.R. Kumar, S.I. Stephens, D. Boehm, C.L. Tsou, J. Shu, A. Bhuiya, M. Armstrong, A.R. Harris, P.Y. Chen, J.M. Osterloh, A. Meyer-Franke, B. Joehnk, K. Walcott, A. Sil, C. Langelier, K.S. Pollard, E.D. Crawford, A. S. Puschnik, M. Phelps, A. Kistler, J.L. DeRisi, J.A. Doudna, D.A. Fletcher, M. Ott, Amplification-free detection of SARS-CoV-2 with CRISPR-Cas13a and mobile phone microscopy, Cell 184 (2) (2021) 323–+.
[36] T. Tian, Z.Q. Qiu, Y.Z. Jiang, D.B. Zhu, X.M. Zhou, Exploiting the orthogonal CRISPR-Cas12a/Cas13a trans-cleavage for dual-gene virus detection using a handheld device, Biosens. Bioelectron. 196 (2022).
[37] Y.D. Ma, K.H. Li, Y.H. Chen, Y.M. Lee, S.T. Chou, Y.Y. Lai, P.C. Huang, H.P. Ma, G. B. Lee, A sample-to-answer, portable platform for rapid detection of pathogens with a smartphone interface, Lab Chip 19 (22) (2019) 3804–3814.
[38] X.L. Chen, G.H. Cao, X.F. Wang, Z. Ji, F.L. Xu, D.Q. Huo, X.G. Luo, C.J. Hou, Terminal deoxynucleotidyl transferase induced activators to unlock the trans-cleavage of CRISPR/Cpf 1 (TdT-IU- CRISPR/Cpf 1): an ultrasensitive biosensor for Dam MTase activity detection, Biosens. Bioelectron. 163 (2020).
[39] S.X. Zhao, J. Huang, J.C. Lei, D.Q. Huo, Q. Huang, J. Tan, Y. Li, C.J. Hou, F.C. Tian, A portable and automatic dual-readout detector integrated with 3D-printed microfluidic nanosensors for rapid carbamate pesticides detection, Sensor. Actuator. B Chem. 346 (2021).